

Rapid Start-Up of the Steam Boiler, Considering the Allowable Rate of Temperature Changes

Jan Taler and Piotr Harchut

*Department of Power Installations, Cracow University of Technology
Poland*

1. Introduction

The development of wind turbine engineering, which can be characterized by large inconsistencies in the amount of delivered electricity over time, generated new problems regarding the regulation of power engineering systems. At high and low wind speeds, the energy production falls rapidly, meaning that the conventional heat or steam-gas blocks have to be activated very quickly. Steam boilers in blocks have to be designed in a way that allows for a start-up of the block within a few dozen minutes. The main elements limiting the quick activation of steam boilers are thick-walled structural elements, in which heat induced stresses can occur during the start-up cycle.

The start-up and the shut-down processes shall be conducted in a way that ensures that the stresses at the places of stress concentration do not exceed the allowable values.

To be able to ensure the appropriate durability and safety of the blocks adapted for a rapid start up, a precise analysis of the flow-heat processes, together with the strength analysis, is required. Such analysis is covered in this paper.

German boiler regulations, TRD - 301 and the European Standard, EN-12952-3 allow determining two allowable rates for heating the pressure element:

- $v_{1,}$ the pressure p_1 at the beginning of the start-up process,
- $v_{2,}$ at the pressure p_2 at the end of the start-up process.

Heating rates for intermediate pressures shall be determined using the method of linear interpolation (Fig. 1).

To be able to heat the boiler evaporator at the maximum allowable rate, heat flow rate \dot{Q}_i shall be delivered to the evaporator in the boiler furnace chamber (Fig. 2). The value of \dot{Q}_i is a function of many parameters, but for the boiler of a specific construction, it depends mainly on the rate of changes of the saturation pressure dp_s / dt and the mass of the saturated steam mass flow rate.

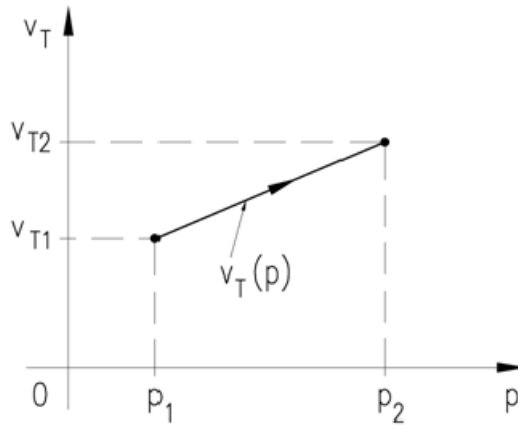


Fig. 1. Heating rate of the pressure boiler element as a pressure function, determined in accordance with TRD-301 regulations.

2. Pressure and temperature changes in the evaporator during the boiler heating process

In accordance with TRD 301 regulations (Fig. 1), the changes of the heating rate $v_t = dT_n/dt$ in the pressure function are interpolated using a straight line.

$$\frac{dT_n}{dt} = \frac{p_2 v_{T1} - p_1 v_{T2}}{p_2 - p_1} + \frac{v_{T2} - v_{T1}}{p_2 - p_1} p_n(T_n) \quad (1)$$

The water saturation pressure $p_n(T_n)$ from Eq. (1) can be expressed in the following way in the temperature function:

$$p_n = \exp(-19,710662 + 4,2367548T_n) \quad (2)$$

Where pressure p_n is expressed in bars and temperature T_n is expressed in °C.

Eq. (1) has been integrated using the Runge-Kutty method of the 4-th rank at the following initial condition:

$$T_n \Big|_{t=0} = T_n(p_1) \quad (3)$$

After determining, by solving the initial condition (1-3), the flow of the saturation temperature in a function of time, that is $T_n(t)$, the pressure changes $p_n(t)$ can be determined, e.g., from function (2). The pressure changes rate dp_n/dt and the saturation temperature changes rate dT_n/dt in a function of time shall be determined on the basis of the assumed run $v_T(p_n)$ (Fig. 1).

In this paper, the dynamics of the boiler evaporator of the OP-210M boiler will be analysed.

OP-210M is a fine coal fuelled boiler with natural circulation. The $T_n(t)$ and $p_n(t)$ flows, determined for $p_1=0$ bar, $v_{T1}=2$ K/min and $p_2=108,7$ bar, $v_{T2}=5$ K/min are presented in Fig. 2.

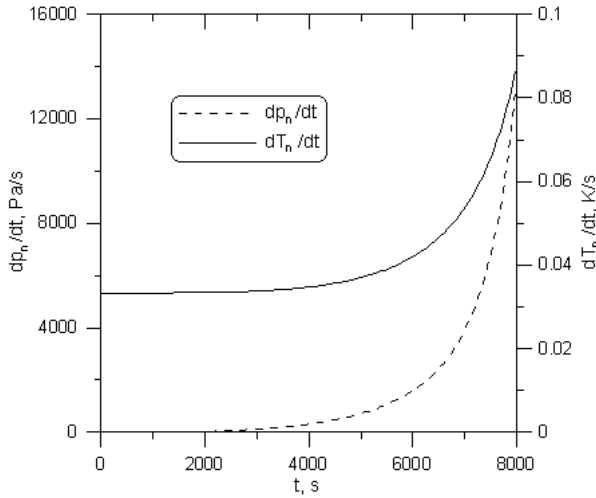


Fig. 2. Temperature and saturation pressure changes in the boiler evaporator during the heating process.

After determining the $T_n(t)$ and dT_n/dt time run, it is possible to determine the rate of pressure changes dp_n/dt using the following formula:

$$\frac{dp_n}{dt} = \frac{dp_n}{dT_n} \frac{dT_n}{dt} \tag{4}$$

Where functions dp_n/dT_n for saturated steam can be determined by the integration of formula (2).

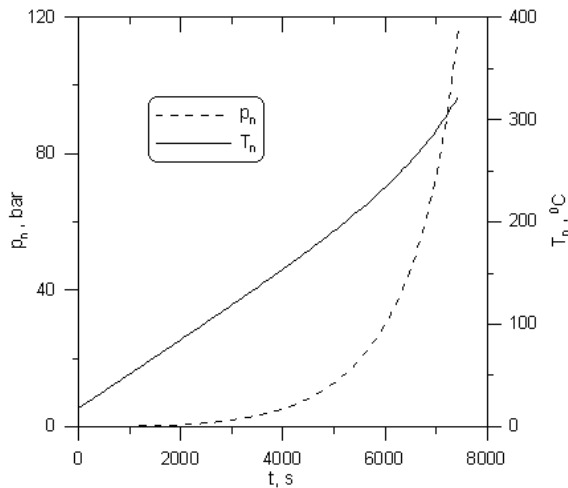


Fig. 3. Rates of the pressure dp_n/dt and temperature dT_n/dt changes, during the evaporator heating process.

The pressure dp_n/dT_n changes rate can also be calculated using an approximate formula:

$$\frac{dp_n}{dt} = \frac{p_n(t + \Delta t) - p_n(t - \Delta t)}{2\Delta t} \quad (5)$$

Where: Δt is the time step.

For the calculations, it can be assumed, for example, that $\Delta t = 1$ s. Temperature dT_n/dt and pressure dp_n/dt changing rates are presented in Fig. 3.

3. Mass and energy balance for the boiler evaporator

Modelling of the transient state effects occurring in the boiler evaporator is usually done while assuming that it is an object having a concentrated mass and heat capacity ⁴. The start point for the determination of the heat flow rate \dot{Q}_k , which assures that the evaporator is heated at the desired rate $vT(t)$, are the mass and energy balance equations for the evaporator (Fig. 4):

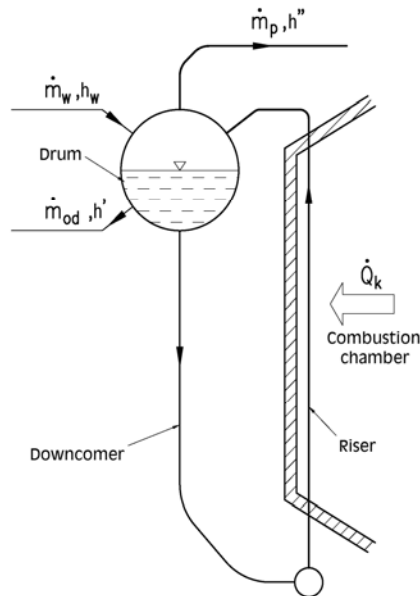


Fig. 4. Diagram of the boiler evaporator.

$$\frac{d(V' \rho' + V'' \rho'')}{d\tau} = \dot{m}_w - \dot{m}_p - \dot{m}_{od} \quad (6)$$

$$\frac{d(V' \rho' + V'' \rho'')}{d\tau} = \dot{m}_w - \dot{m}_p - \dot{m}_{od} \quad (7)$$

After transforming formulas (6) and (7) we obtain:

$$\begin{aligned} \dot{Q}_k = & \dot{m}_{od} \frac{\rho''}{\rho' - \rho''} (h'' - h') - \dot{m}_w \left(h_w - \frac{\rho' h' - \rho'' h''}{\rho' - \rho''} \right) + \dot{m}_p \frac{\rho' (h'' - h')}{\rho' - \rho''} + \\ & [V' \left(\rho' \frac{dh'}{dp} + \frac{\rho'' (h'' - h')}{\rho' - \rho''} \frac{d\rho'}{dp} - 1 \right) + V'' \left(\rho'' \frac{dh''}{dp} + \frac{\rho' (h'' - h')}{\rho' - \rho''} \frac{d\rho''}{dp} - 1 \right) + m_{cm} \frac{dT_n}{dp_n}] \frac{dp_n}{dt} \end{aligned} \quad (8)$$

Formula (8) allows determining the heat flow rate \dot{Q}_k , which shall be delivered to the evaporator from the furnace chamber in order to ensure the assumed rate of the pressure change dp_n/dt . Changes of the $d\rho'/dp$ and $d\rho''/dp$ functions and the dh'/dp and dh''/dp functions, appearing in formula (8) are presented in Fig. 5 and Fig. 6.

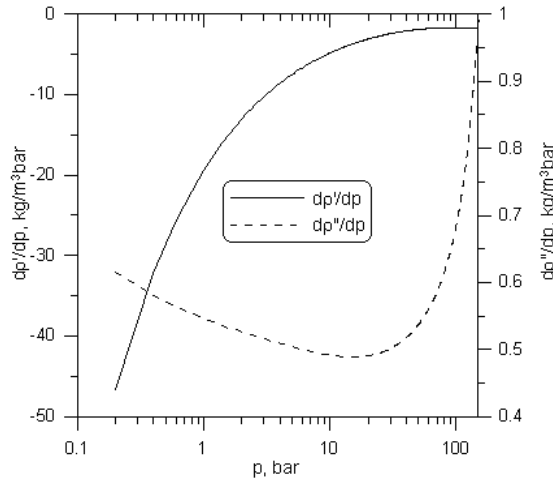


Fig. 5. Changes of the $d\rho'/dp$ and $d\rho''/dp$ derivatives as a function of pressure.

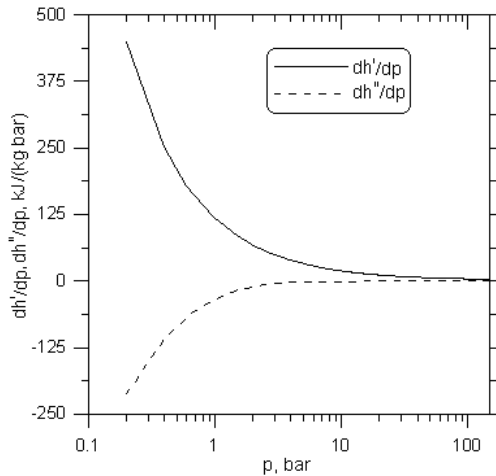


Fig. 6. Changes of the dh'/dp i dh''/dp derivatives as a function of pressure.

The precision in determining those functions is very important. The best way is to determine those functions through analytical differentiation of the $\rho'(p)$ and $\rho''(p)$ functions, obtained earlier using the least square methods on the basis of the pair tables.

4. Heat flow rate absorbed in combustion chamber

From the conducted calculations, we can see, that the heat flow rate \dot{Q}_i delivered to the evaporator can be lowered significantly by reducing the mass of the steam mass flow rate \dot{m}_p delivered from the boiler drum. The minimum steam mass flow rate \dot{m}_p , which shall be produced in the boiler during the start-up process can be determined from the condition, stating that the maximum allowable temperatures for the particular stages of the heater shall not be exceeded. The furnace oil mass flow rate \dot{m}_{pal} , delivered to the burners during the boiler start up process, which is necessary to assure the heat flow rate \dot{Q}_i shall be determined on the basis of the calculations of the boiler furnace chamber.

The heat flow rate $\dot{Q}_{k, kom}$ absorbed by the walls of the boiler furnace chamber, expressed in W , can be calculated from the following formula:

$$\dot{Q}_{k, kom} = \dot{m}_{pal} W_d + \dot{m}_{pow} c_{p, pow} \Big|_0^{T_{pow}} T_{pow} - \dot{m}_{sp} c_{p, sp} \Big|_0^{T_{sp}''} T_{sp}'' \quad (9)$$

- \dot{m}_{pal} – fuel mass flow rate, kg/s,
- W_d – fuel calorific value, J/kg,
- \dot{m}_{pow} – air mass flow rate, kg/s,
- $c_{p, pow} \Big|_0^{T_{pow}}$ – average specific heat of air, at constant pressure and at temperature from 0 to T_{pow} [°C], J/(kg·K)
- T_{pow} – temperature of air delivered to the furnace chamber, °C
- \dot{m}_{sp} – flue gas mass flow rate, kg/s
- $c_{p, sp} \Big|_0^{T_{sp}''}$ – average specific heat of flue gas, at constant pressure and at temperature from 0 to T_{sp}'' [°C], J/(kg·K)
- T_{sp}'' – flue gas temperature at the exit of the furnace chamber, °C

The temperature of flue gases at the exit of the furnace chamber, T_{sp}'' is calculated from the equation:

$$T_{sp}'' = \frac{T_{ad} + 273,15}{M \left(\frac{a_p}{Bo} \right)^{0,6} + 1} - 273,15 \quad (10)$$

Where Bo is the Boltzmann number, determined by the formula:

$$Bo = \frac{\dot{m}_{sp} \bar{c}_{p, sp}}{\sigma \psi A_k T_{ad}^3} \quad (11)$$

$\bar{c}_{p,sp}$ is the average specific heat of flue gases in J/(kg · K), at temperature ranging from T''_p to T_{ad}

$$\bar{c}_{p,sp} = c_{p,sp} \left| \frac{T_{ad}-273,15}{T''_p-273,15} \right. \tag{12}$$

- a_p - emissivity of the furnace chamber,
- M - parameter characterizing the area, in which the flame temperature in the chamber is highest,
- A_k - area of the walls of the boiler furnace chamber, m²
- T_{ad} - theoretical (adiabatic) combustion temperature, °C
- σ - Stefan-Boltzmann constant, $\sigma = 5,67 \cdot 10^{-8} \text{ W}/(\text{m}^2 \cdot \text{K}^4)$
- ψ - thermal efficiency coefficient of the screens, being the quotient of the heat flux absorbed by the screen and the incident flux.

The calculation of the heat flow rate $\dot{Q}_{k, kom}$ absorbed by the walls of the furnace chamber of the OP-210M boiler has been calculated using (9). In the function of the fuel mass flow rate \dot{m}_{pal} and the air excess coefficient λ , the calorific value of the oil was assumed to be: $W_d = 41060 \text{ kJ/kg}$.

The results of the calculations are presented in Fig. 7.

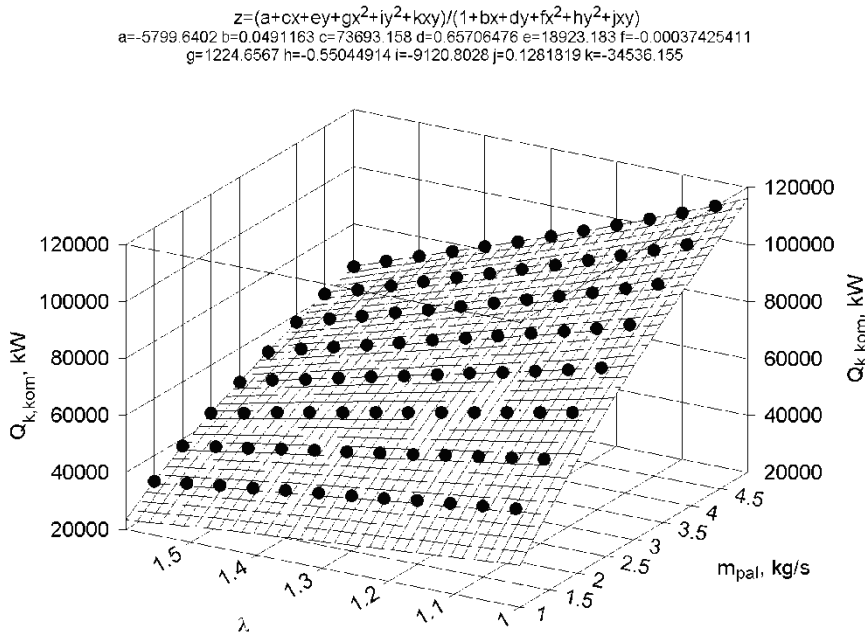


Fig. 7. Heat flow rate $\dot{Q}_{k, kom}$, in kW, delivered to the evaporator of the OP-210M boiler, as a function of the fuel mass flow rate \dot{m}_{pal} in kg/s and the air excess coefficient λ .

It was proven that the increase of the air excess coefficient λ at the assumed fuel mass flow rate \dot{m}_{pal} leads to the reduction of the heat flux delivered from flue gases in the furnace chamber to the evaporator. This is due to the fact that the temperature of the flue gases in the furnace chamber T_{pl} was lowered significantly, which in turn led to a significant decrease of the heat flow rate $\dot{Q}_{k,kom}$, as the heat flux is proportional to temperature difference between the flame temperature and the temperature of the chamber walls raised to the fourth power, that is $(T_{pl}^4 - T_{sc}^4)$ when λ increases $\dot{Q}_{k,kom}$ is reduced, and the heat flux absorbed by the steam over heaters increases. Increasing the fuel mass flow rate \dot{m}_{pal} at the assumed air excess coefficient λ leads to the increase of the heat flow rate $\dot{Q}_{k,kom}$ absorbed by the walls of the furnace chamber.

Next, the fuel mass flow rate \dot{m}_{pal} delivered to the boiler during the start-up (heating) process was determined. After determining from (8) the heat flow rate $\dot{Q}_k(t)$, the non-linear algebraic equation is solved.

$$\dot{Q}_k(t) = \dot{Q}_{k,kom}(\dot{m}_{pal}, \lambda) \quad (13)$$

\dot{m}_p, \dot{m}_{pal} The fuel mass flow rate, at the assumed value of the air excess coefficient λ , is determined from (13). Changes of the mass flow rate in a time function, during the start-up process of the OP-210M boiler, determined from (13), for $\lambda = 1,1$ is presented in Fig. 9a and 9b. The calculations were conducted for different steam mass flows produced in the boiler evaporator. The mass of the fuel oil used for the boiler start up process from time $t=0$ to $t=t_k$ can be calculated using the formula:

$$m_{pal} = \int_0^{t_k} \dot{m}_{pal} dt \quad (14)$$

The integral (14) was calculated numerically, using the trapezium rule for integration.

5. Calculation results

The calculation has been completed for the evaporator of the OP-210M boiler, for the pressure change rate dp_n/dt presented in Fig. 3. The temperature of the incoming water T_w during the evaporator heating process is at a given moment lower by 10K than the saturation temperature T_n . The temperature run of the incoming water T_w , the saturation temperature T_n and the pressure in the evaporator p_n are presented in Fig. 8.

The calculations have been conducted for the following data:

$$\dot{m}_{ods} = 0,51 \text{ kg/s}, \quad \dot{m}_w = 17,1 \text{ kg/s}, \quad \dot{m}_p = 16,57 \text{ kg/s}, \quad m_m = 171900 \text{ kg}, \quad c_m = 511 \text{ J/(kg}\cdot\text{K)}, \\ V' = 43,6 \text{ m}^3, \quad V'' = 15,9 \text{ m}^3.$$

The results of the \dot{Q}_k calculations, determined for various saturated steam mass flow rates, are presented in Fig. 9a and Fig. 9b.

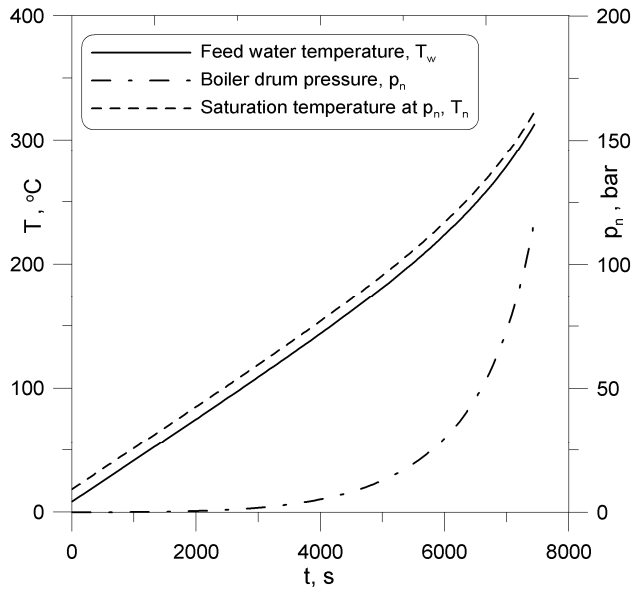
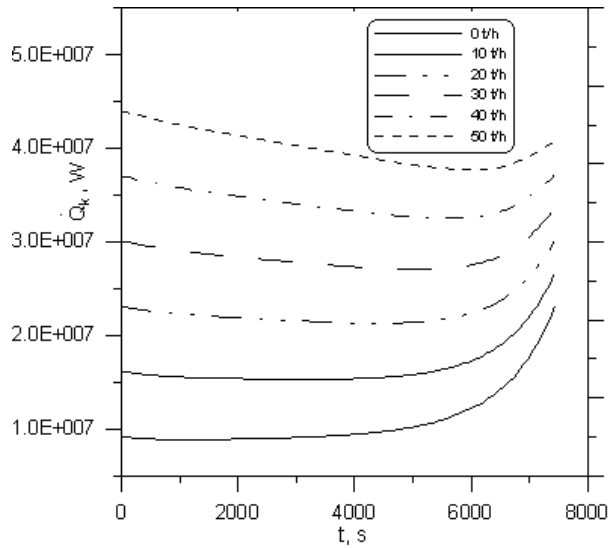


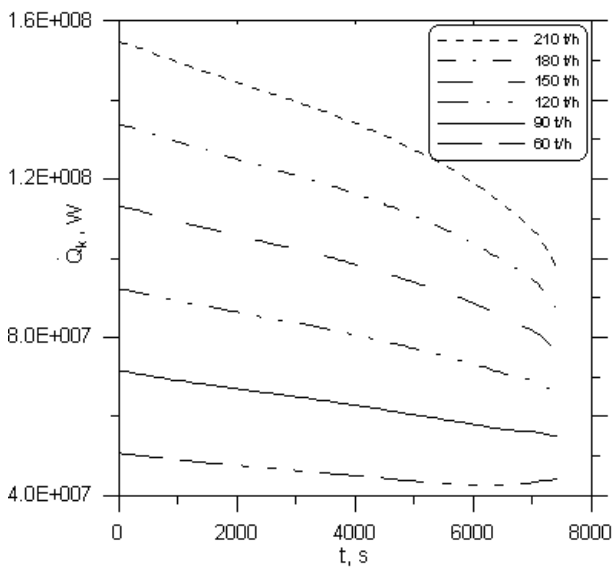
Fig. 8. Temperature run of the incoming water temperature T_w , saturation temperature T_n and pressure in the evaporator p_n during the boiler start up cycle.

After analysing the results shown in Fig. 9a we can see that if the mass capacity of the evaporator \dot{m}_p equals zero, then the flow rate of the heat flow rate \dot{Q}_i delivered to the evaporator shall increase. In this case, all heat delivered from the furnace chamber is used mainly for heating water contained in the boiler evaporator. This is due to the increase of the specific heat of water c_w , which increases in line with the pressure increase. For example, at pressure $p_n=1$ MPa water specific heat equals: $c_w = 4405$ J/(kg·K), and at the pressure $p_n=10$ MPa water specific heat equals: $c_w = 6127$ J/(kg·K). Moreover, at the end of the start-up process a large increase of the rate of temperature changes in the evaporator was noticed (Fig. 3), which required increased heat flow rate \dot{Q}_i to be delivered to the evaporator.

In larger mass capacities \dot{m}_p the heat flow rate \dot{Q}_i , which shall be delivered from the furnace chamber to the evaporator, increases significantly, because there is a large power demand on water evaporation (Fig. 9). For the evaporator efficiencies greater than 90 t/h (Fig. 9b), however, it has been noted that for the assumed flux \dot{m}_p , the reduction of the heat flow rate \dot{Q}_i occurred during the end phase of the heating process, despite the increase of the rate of evaporator heating (Fig. 3). This is due to the fact that the water evaporation heat, $r = h'' - h'$ decreases in line with the pressure increase in the evaporator. For example, at the pressure $p_n=1$ MPa, water evaporation heat equals: $r = 2014,4$ J/(kg·K), and at the pressure $p_n=10$ MPa, the water evaporation heat is reduced to: $r = 1317,7$ J/(kg·K).



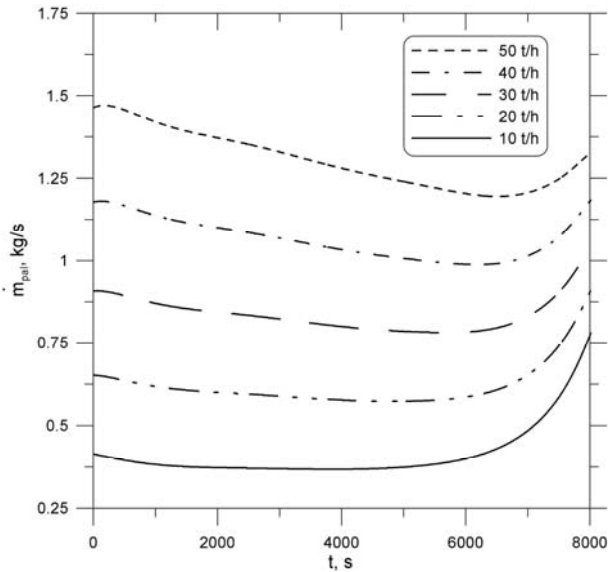
a)



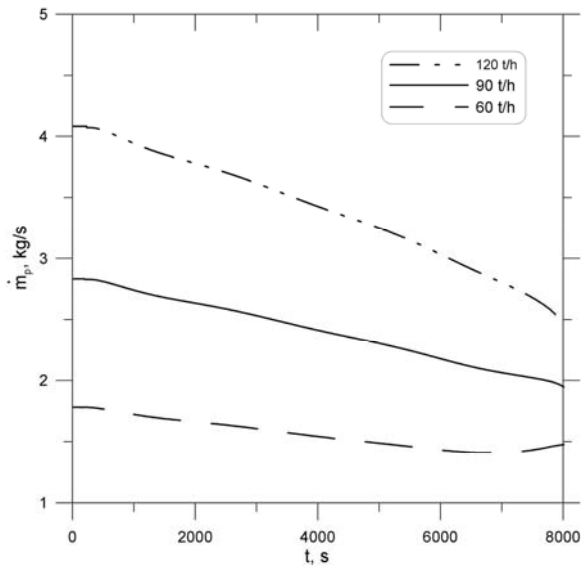
b)

Fig. 9. Heat flow rate \dot{Q}_k delivered to the evaporator of the boiler in the furnace chamber for various steam fluxes \dot{m}_p .

Fuel mass flow rate \dot{m}_{pal} during the start-up of the OP-210M boiler obtained from Eq. (13) for the excess air number $\lambda=1,1$ are shown in Figs. 10a and 10b.



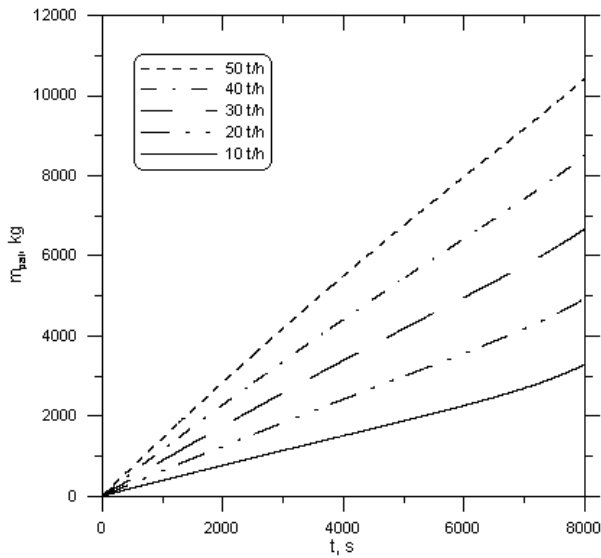
a)



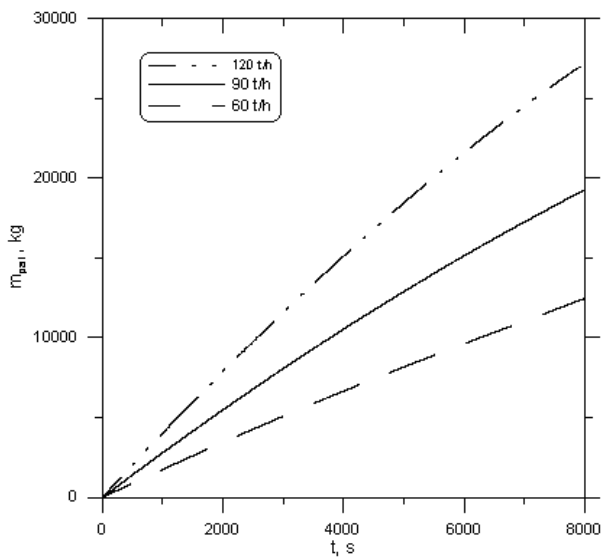
b)

Fig. 10. Changes of the fuel mass flow rate \dot{m}_{fuel} in kg/s, during the start-up of the OP-210M boiler, depending on the steam mass flow rate \dot{m}_p in t/h, produced in the boiler evaporator.

The calculations are carried out for various steam flow rates \dot{m}_p generated in the evaporator.



a)



b)

Fig. 11. Fuel consumption m_{pal} , in kg, during the start-up process of the OP-210M boiler, depending on the steam mass flow rate \dot{m}_p , in t/h, produced in the boiler evaporator.

The results of the calculations of m_{pal} corresponding to the runs of the fuel mass flow rates \dot{m}_{pal} from Fig. 10 are presented in Fig. 11.

From the analysis of the results shown in Fig. 11 we can see that the fuel consumption depends mainly on the steam mass flow rate \dot{m}_p removed from the boiler drum. During the start-up process, lasting 8000s, the fuel consumption varies from $m_{pal} = 3308$ kg, at the steam mass flow rate $\dot{m}_p = 10$ t/h, to $m_{pal} = 27207$ kg, at the steam mass flow $\dot{m}_p = 120$ t/h. Due to the high price of the fuel oil, the boiler start up process shall be conducted at the minimum steam mass flow rate \dot{m}_p , ensuring the appropriate cooling of the pipes of the over heaters.

Strength analyses show that temperature can change at the beginning of warm-up by leaps and bounds, without exceeding the allowable stress.

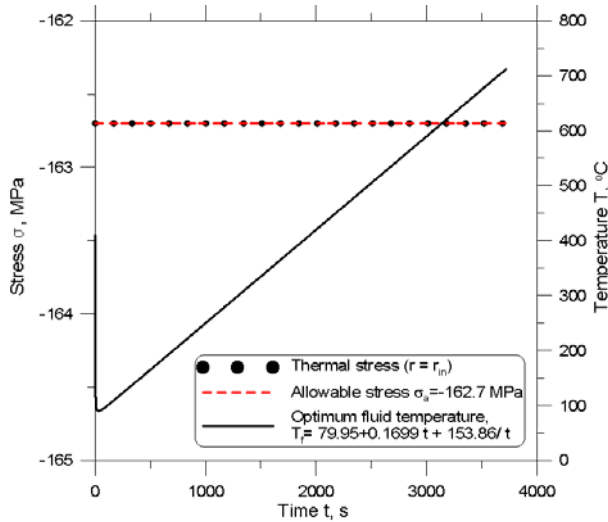


Fig. 12. The allowable process of the temperature due to the thermal stresses on the inner surface of the boiler drum.

The allowable temperature of the process due to the thermal stresses on the inner surface of the drum can be approximated by using:

$$T_n(t) = a + bt + \frac{c}{t^2} \tag{15}$$

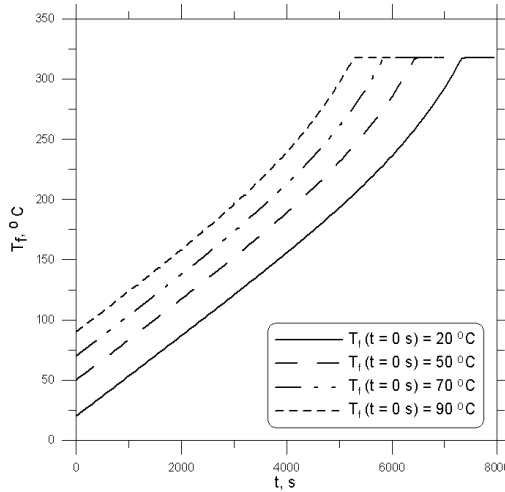
where the constants a , b and c are determined from the condition:

$$\sigma_\varphi(r_m, t_i) \cong \sigma_a \quad t_i = (i - 1)\Delta t \quad i = 1, 2, 3, \dots, n \tag{16}$$

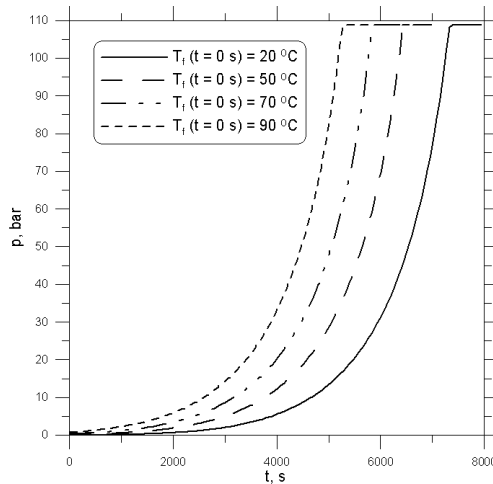
Condition (16) means that for optimal temperature of the process defined by formula (15) constants a , b and c should be chosen so that the thermal stress on the inner circumferential surface of the drum was, for n time points, equal to the allowable stress. In the case of the drum analysed in this paper, for allowable stress $\sigma_a = -162,7$ MPa, the following constants were obtained: $a=79,95^\circ\text{C}$, $b=0,1699$ °C/s, $c=153,86$ s. Starting with an optimal start-up boiler water temperature change in the drum is very difficult, because the optimal temperature is very high at the beginning of start-up and then very quickly reduced to the minimum value.

Therefore, during start-up an approximation of optimal temperature change will be implemented by the step up temperature increase at the beginning and then heating at a constant speed. When the pressure in the drum is higher than the atmospheric pressure, after the jump of temperature, the speed of temperature change is equal v_{T1} (at the beginning) and v_{T2} (at the end of start-up). Determination of the heating or cooling rate of the drum for any pressure p is the same as in TRD 301 regulations or European Standard BS EN 12952-3.

Fig. 13a and fig. 13b show the changes in temperature and pressure of water in the drum at different initial temperature jumps.



a)



b)

Fig. 13. Temperature and pressure of the water in the drum during boiler start-up.

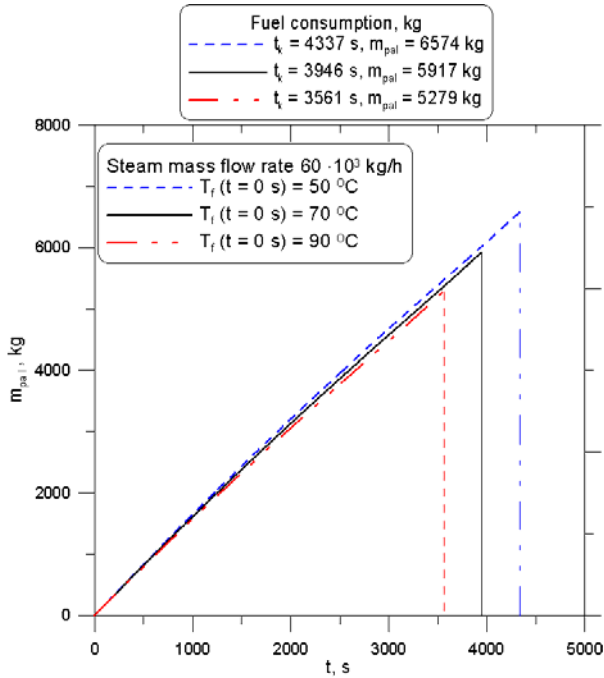


Fig. 14. Fuel consumption and boiler start-up time at different initial jumping changes in water temperature in the evaporator boiler.

An analysis of the results in Fig. 14 shows that the release of the initial jump in the temperature of the boiler start-up reduces the time and reduces fuel consumption.

6. Conclusions

The model of the dynamics of the boiler evaporator, presented in this paper, can be used for the determination of the heat flux, flowing from flue gases in the furnace chamber to the boiler evaporator, necessary to warm up the boiler at the assumed rate of the medium temperature change in the boiler evaporator. The fuel mass flow rate \dot{m}_{pal} , for which the heat flux delivered to the evaporator equals \dot{Q}_i , is determined on the basis of the calculations of the boiler furnace chamber. Fuel consumption during the boiler start up process, necessary for heating the boiler evaporator to the assumed temperature, from the assumed nominal start temperature, assuming that the heating of the boiler drum is conducted at the maximum allowable speed, due to the limitations caused by heat stresses at the boiler drum/down comers intersection, has been determined. In order to limit the consumption of the expensive fuel oil during the boiler start up process, the process shall be conducted at the minimum steam mass flow rate, ensuring the appropriate cooling of the over heaters and at the minimum allowable air coefficient. The dependencies derived in this paper can be used for the preparation of the optimal technology of the boiler start up process.

It is shown that allowing the rapid increase of water temperature at the start of commissioning of the boiler reduces the boiler start-up time and helps to reduce fuel oil consumption.

7. References

- TRD 301 (2001), Zylinderschalen unter innerem Überdruck. *Technische Regeln für Dampfkessel (TRD)*, pp. 143-185, Heymanns Beuth Köln – Berlin, Germany.
- Staff Report, (2007). Dealing with cycling: TRD 301 and the Euro Norm compared, *Modern Power Systems*, Vol 27, No 5, p 33-38.
- European Standard, EN 12952-3, *Water-tube boilers and auxiliary installations – Part 3: Design and calculation for pressure parts*, CEN – European Committee for Standardization, rue de Stassart 36, B-1050 Brussels, 25. July 2001.
- Profos, P., (1962). *Die Regelung von Dampfanlagen*, Springer, Berlin, Germany.
- Styrykowicz, M. A., Katkowskaja, K. J., Sierow, E. P. (1959). *Kotielnyje agregaty*. Gosenergoizdat, Moscow, Russia.
- Sierow, E.P., Korolkow, B. P. (1981). *Dinamika parogienieratorow*. Energija, Moscow, Russia.
- Taler, J., Dzierwa, P. (2010): A new method for optimum heating of steam boiler pressure components. *International Journal of Energy Research*, Volume 35, Issue 10, pages 897-908, Wiley, August 2011.

© 2012 The Author(s). Licensee IntechOpen. This is an open access article distributed under the terms of the [Creative Commons Attribution 3.0 License](#), which permits unrestricted use, distribution, and reproduction in any medium, provided the original work is properly cited.